

# Spatiotemporal neural interactions underlying continuous drawing movements as revealed by magnetoencephalography

Vassilios N. Christopoulos · Arthur C. Leuthold ·  
Apostolos P. Georgopoulos

Received: 24 April 2012 / Accepted: 23 July 2012 / Published online: 25 August 2012  
© Springer-Verlag (outside the USA) 2012

**Abstract** Continuous and sequential movements are controlled by widely distributed brain regions. A series of studies have contributed to understanding the functional role of these regions in a variety of visuomotor tasks. However, little is known about the neural interactions underpinning continuous movements. In the current study, we examine the spatiotemporal neural interactions underlying continuous drawing movements and the association of them with behavioral components. We conducted an experiment in which subjects copied a pentagon continuously for ~45 s using an XY joystick, while neuromagnetic fluxes were recorded from their head using a 248-sensor whole-head magnetoencephalography (MEG) device. Each sensor time series was rendered stationary and non-autocorrelated by applying an autoregressive integrated moving average model and taking the residuals.

We used the directional variability of the movement as a behavioral measure of the controls generated. The main objective of this study was to assess the relation between neural interactions and the variability of movement direction. That is, we divided the continuous recordings into consecutive periods (i.e., time-bins) of 51 steps duration and computed the pairwise cross-correlations between the prewhitened time series in each time-bin. The circular standard deviation of the movement direction within each time-bin provides an estimate of the directional variability of the 51-ms trajectory segment. We looked at the association between neural interactions and variability of movement direction, separately for each pair of sensors, by running a cross-correlation analysis between the strength of the MEG pairwise cross-correlations and the circular standard deviations. We identified two types of neuronal networks: in one, the neural interactions are correlated with the directional variability of the movement at negative time-lags (feedforward), and in the other, the neural interactions are correlated with the directional variability of the movement at positive time-lags (feedback). Sensors associated mostly with feedforward processes are distributed in the left hemisphere and the right occipital–temporal junction, whereas sensors related to feedback processes are distributed in the right hemisphere and the left cerebellar hemisphere. These results are in line with findings from a series of previous studies showing that specific brain regions are involved in feedforward and feedback control processes to plan, perform, and correct movements. Additionally, we looked at whether changes in movement direction modulate the neural interactions. Interestingly, we found a preponderance of sensors associated with changes in movement direction over the right hemisphere—ipsilateral to the moving hand. These sensors exhibit stronger coupling with the rest of the sensors for

---

V. N. Christopoulos · A. C. Leuthold · A. P. Georgopoulos (✉)  
Brain Sciences Center (11B), Veterans Affairs Medical Center,  
VAHCS, One Veterans Drive, Minneapolis, MN 55417, USA  
e-mail: omega@umn.edu

V. N. Christopoulos  
Department of Computer Science and Engineering,  
University of Minnesota, Minneapolis, MN 55455, USA

*Present Address:*  
V. N. Christopoulos  
Division of Biology, California Institute of Technology,  
Mail Cole 216-76, Pasadena, CA 91125, USA

V. N. Christopoulos · A. P. Georgopoulos  
Center for Cognitive Sciences, University of Minnesota Medical  
School, Minneapolis, MN 55455, USA

A. C. Leuthold · A. P. Georgopoulos  
Department of Neuroscience, University of Minnesota Medical  
School, Minneapolis, MN 55455, USA

trajectory segments with high rather than low directional movement variability. We interpret these results as evidence that ipsilateral cortical regions are recruited for continuous movements when the curvature of the trajectory increases. To the best of our knowledge, this is the first study that shows how neural interactions are associated with a behavioral control parameter in continuous and sequential movements.

**Keywords** Magnetoencephalography · Neural interactions · Directional variability of movement · Feedforward–feedback motor control

## Introduction

In daily life, humans are capable of performing a diverse variety of movements. Some of them are executed automatically (e.g., reflexes), whereas others are more complex and produced by combining multiple discrete movements in a proper sequence. The question of how the brain generates a sequence of actions to achieve a certain behavioral goal, such as writing, driving vehicles, and navigating around a city, is a topic of many research studies. Electrophysiological studies in non-human primates and clinical studies in patients with brain damage have contributed greatly to understanding the role of distinct cortical regions in continuous and sequential movements (Luria and Tsvetkova 1964; De Renzi 1982; Averbeck et al. 2003, 2009; see review from Caminiti et al. 2010). Despite the significant contribution of these studies, they are limited in exploring only specific brain regions. To gain a better understanding of the neural mechanisms underlying continuous and sequential movements, we need to understand not only the functional properties of these areas, but also their connectivity and the spatiotemporal interactions among them. Modern neuroimaging studies, such as magnetoencephalography (MEG), provide the technology to gather simultaneous activity across the whole brain, acquiring a global perspective on the dynamic networks established in the brain.

A number of studies have used neuroimaging techniques to explore the characteristics of dynamic brain networks established in a variety of motor control tasks, such as self-paced finger extensions (Gerloff et al. 1998), simple finger movements with different rates (Toma et al. 2002), reaching (Gevins et al. 1983), grasping (Grol et al. 2007), sequences of bimanual movements (Andres et al. 1999), and copying of geometrical shapes (Leuthold et al. 2005). Although such experiments have contributed to formulate the idea that large cortical networks interact and communicate to generate movements, they do not address the question of how cortical interactions are related to

behavioral control parameters of the tasks. In the current study, we explore the association between neural interactions and behavioral control parameters in a continuous and sequential movement task. We conducted an experiment in which subjects were instructed to copy continuously a pentagon using an XY joystick, while neuromagnetic fluxes were recorded from their head using a 248-sensor whole-head MEG device. In drawing a copy of the pentagon, the subjects should generate a sequence of straight and curved movements to represent the sides and the corners of the shape, respectively, in a proper spatial relationship. Therefore, we consider the changes in the movement direction as a behavioral control parameter of the task. The goal of this study is to assess how neural interactions vary with changes in movement direction. Our hypothesis is that motor behavior occurs along a continuum of feedforward and feedback control schemes. That is, when you intend to change direction, the sensorimotor system generates appropriate control signals for changing movement direction (forward) and uses mechanisms to monitor and correct that change (feedback).

To test this hypothesis, we assessed the relation between neural interactions and variability of movement direction. We used Box–Jenkins time series analysis (Box et al. 2008) to remove confounding autocorrelations and trends from the MEG raw data. We divided the continuous recording into consecutive time-bins of 51 ms and computed the cross-correlations between pairs of sensors over  $\pm 25$  time-lags including zero ( $\sim 51$  ms) within each time-bin. This number of lags was chosen because we were interested in short-range neural interactions. We assessed the relation between neural interactions and directional variability of movement by performing a cross-correlation analysis between the strength of the peak MEG cross-correlations and the circular standard deviations across all pairs of sensors and subjects.

In accordance with our hypothesis, the results showed that interactions between brain regions vary with the directional variability of the movement in a feedforward–feedback control scheme. We found interactions in networks of MEG sensors that are correlated with the directional variability of movement at negative (forward) and positive (feedback) time-lags. The sensors that are mainly involved in feedforward networks are distributed in the left hemisphere and the right occipital–temporal junctions. On the other hand, the sensors that are mostly involved in feedback networks are located in the right hemisphere and the left cerebellar hemisphere. These results are consistent with a series of studies showing that specific cortical and subcortical regions are involved in feedforward and feedback control processes in generating movements (Desmurget and Grafton 2000; Shadmehr and Krakauer 2008). However, the novelty of our study is that

we characterized the feedforward and feedback control mechanisms not by measuring the activity of particular brain regions but by looking at the “whole” brain and relating the neural interactions with a behavioral control parameter.

We were also interested in testing whether there are any differences in the pattern of neural interactions between straight and curved movements. To test that, we assigned all trajectory segments into two groups based on their circular standard deviation—trajectory segments with low (group 1) and high (group 2) directional variability—and performed a two-sample *t* test analysis between the pairwise MEG cross-correlations of the two groups. We identified pairs of sensors located in the right hemisphere—ipsilateral to the moving hand—that have different coupling strengths between the two groups. These sensors exhibited stronger coupling with the rest of the sensors for curved than straight trajectory segments. Although this finding may seem counterintuitive, it complements other studies which suggested that ipsilateral brain areas are recruited for movements with higher indices of difficulty (Rao et al. 1993; Salmelin et al. 1995; Seidler et al. 2004).

## Methods

The data for this analysis are subset of a dataset from a previous study conducted in our laboratory (Leuthold et al. 2005). In the following, we give a brief description of the experimental paradigm, the data acquisition, and the data preprocessing (for more information see Leuthold et al. 2005).

### Subjects

Ten healthy right-handed subjects (23–41 years old, 5 men and 5 women) with normal or corrected-to-normal vision and with no known neurological or physical dysfunction participated in the MEG imaging study for monetary compensation. The appropriate institutional review board approved the study protocol, and informed consent was obtained prior to the study based on the Declaration of Helsinki. All subjects denied any history of neurological or psychiatric illness, including drug/alcohol abuse. Additionally, no subjects had abnormal neurological magnetic resonance imaging (MRI) studies.

### Experimental paradigm

#### Task

Subjects were instructed to copy the outline of a pentagon continuously using an XY joystick with the right hand,

while fixating on a spot of green light on the center of the pentagon. They copied the pentagon counterclockwise at their own speed without visual feedback of the joystick movement.

#### Experimental set-up

The task stimulus was generated by a computer and was presented on a display 62 cm in front of the subjects, using a liquid crystal display (LCD) project and a periscopic mirror system. The 2-D pentagon displayed subtended approximately 10° of visual angle. The subjects lay supine in the recording chamber having their head inside the cryogenic helmet-shaped Dewar. They copied the pentagon using a 2-D joystick (joystick model 541 FP, Measurement Systems, Norwalk, CT; remodeled by removing all the magnetic parts). The joystick was placed on a rectangular plastic sheet ( $22.6 \times 19.5$ ) cm<sup>2</sup> and raised 3.5 cm above the resting bed and tilted at an angle of 30.6°.

#### Data acquisition

#### Magnetoencephalography (MEG)

Brain activity was recorded using a 248-sensor whole-head axial gradiometer MEG system (Magnes 3600 WH, 4-D neuroimaging, San Diego, CA, USA). The cryogenic helmet-shaped Dewar of the MEG system was located inside a shielded room that reduced electromagnetic and environmental noise. The MEG data were recorded at 1,017.25 Hz and filtered down to 0.1–400 Hz during acquisition.

#### Hand movement

The XY position of the joystick was sampled synchronously at the same rate as the MEG signals (i.e., 1,017.25 Hz) and incorporated directly into the MEG data file to ensure correct time alignment.

#### Data analysis

#### Preprocessing

The MEG data were 248 time series with ~45,000 values per sensor per subject. The obstructive cardiac artifact was removed from the MEG data using the event-synchronous subtraction method (Leuthold 2003).

#### Prewhitening

Neurophysiological time series often are not stationary with respect to their mean and variance and in many cases are dominated by trends, which should be recognized

before any further analysis is done. Since we were interested in assessing the interactions between the sensor time series by calculating the cross-correlation function (CCF), it is required, from first principles (Jenkins and Watts 1968; Granger and Newbold 1974, 1977; Priestley 1981; Box et al. 2008), that individual series be rendered stationary and non-autocorrelated for their cross-correlation to be valid (i.e., not spurious) assessments of these interactions. Stationarity implies that statistical parameters do not vary along the time series—that is, they are invariant under translations of the time axis; and lack of significant autocorrelation is indicated by a practically flat autocorrelogram of the series. For that purpose, we used autoregressive integrated moving average (ARIMA) modeling to remove any autocorrelation and possible trends in the recorded MEG data (“prewhitening” the MEG time series). Building on previous studies, we found that an ARIMA(25,1,1) model was adequate to obtain quasi-stationary time series.

### MEG cross-correlation analysis

To study the spatiotemporal neural interactions, we divided the prewhitened MEG time series into  $N$  time-bins of length 51 time-steps ( $\sim 51$  ms) and performed a cross-correlation analysis between all possible pairs of sensors, within each time-bin, over  $\pm 25$  time-lags ( $\sim 51$  ms—1 lag is equivalent to 0.983 ms, as the sampling frequency is 1,017.25 Hz) including zero-lag. This number of lags was chosen because we are interested in relative short-range neural interactions. The cross-correlation analysis was performed using the IMSL statistical routine DCCF (Compaq Visual Fortran Professional Edition, version 6.6B). We normalized the distribution of the pairwise cross-correlation before averaging across subjects using Fisher’s  $z$ -transformation, Eq. (1).

$$z_{ij}(t) = \frac{1}{2} [\ln(1 + cc_{ij}(t)) - \ln(1 - cc_{ij}(t))] \quad (1)$$

where  $cc_{ij}(t)$  is the pairwise cross-correlation between sensor  $i$  and  $j$  at time-lag  $t$ .

To characterize the cross-correlogram, we computed the sign and the strength of the peak cross-correlation  $z_{ij}(t_{\text{peak}})$ , and the time-lag  $t_{\text{peak}}$  at which the peak occurred. Hence,  $30,628 \times N \times 10$  (where  $N$  is the number of time-bins and 10 the total number of subjects) peak of cross-correlations  $z_{ij}(t_{\text{peak}})$  with the corresponding  $t_{\text{peak}}$  were available for further analysis.

### Movement data

The XY output of the joystick was smoothed using cubic spline approximation to reduce noise from the joystick. To measure the variability of the movement direction

within each time-bin, we computed the circular standard deviation  $\bar{S}$  of each 51-ms trajectory segment as follows:

$$\bar{S} = \sqrt{-2 \ln \bar{R}},$$

$$\bar{R} = \frac{1}{M} \sqrt{\left( \sum_{t=1}^M \cos \theta_t \right)^2 + \left( \sum_{t=1}^M \sin \theta_t \right)^2} \quad (2)$$

where  $M$  is the length of the time-bin (51 ms) and  $\theta_t$  is the instantaneous direction of the movement at any time  $t$ —the lower the circular standard deviation, the lower the variability of movement direction. For example, the circular standard deviations of the “green” and “red” 51-ms-long segments of the movement trajectory in Fig. 1 are 4.9848 and 35.4538, respectively.

### Analysis of the relation between neural interactions and variability of movement direction

We assessed the relation between neural interactions and variability of movement direction, separately for each pair of sensors, performing cross-correlation analysis between the time series of the strength of the peak MEG cross-correlations  $z_{ij}(t_{\text{peak}})$  and the time series of the circular standard deviations  $\bar{S}$ . The flowchart of the analysis is presented in Fig. 2. The time series of  $\bar{S}$  were not stationary for all subjects, and for that reason we applied an ARIMA model to remove the autocorrelation structure of the circular standard deviation time series. After extensive ARIMA modeling and diagnostic checking, including the computation and evaluation of the autocorrelation function (ACF) and the partial autocorrelation function (PACF) of the residuals, we found that ARIMA(10,1,0) was adequate to yield quasi-stationary residuals. The time series of  $z_{ij}(t_{\text{peak}})$  were quasi-stationary and did not require ARIMA modeling. We performed the cross-correlation analysis within  $\pm 3$  time-lags, including zero (note that 1 time-lag corresponds to  $\pm 25$  time-lags in the cross-correlation analysis between the stationary time series of the MEG signals). We chose this time-lag based on findings from previous studies, which showed that the time-lag between neural activity and hand movement varies with the curvature of the movement trajectory from 0 to 200 ms (Moran and Schwartz 1999a, b; Wu et al. 2006).

This analysis yielded 30,268 cross-correlograms, by which the relation between the MEG signal interactions and the variability of movement direction was quantified and summarized by measuring the peak of the cross-correlogram and the time-lag at which the peak occurred. The peak of the cross-correlogram indicates the strength of the coupling between MEG signal interactions and the directional variability of the movement. However, in this analysis, we focused on the time-lag at which the peak of

**Fig. 1** Illustration of two 51-ms-long segments (out of ~45 s total) of the movement trajectory with low (*green segment*) and high (*red segment*) circular standard deviation ( $S_{\text{low}} = 4.9848$ ,  $S_{\text{high}} = 35.4538$ ). *Black arrows* indicate the instantaneous direction of the movement

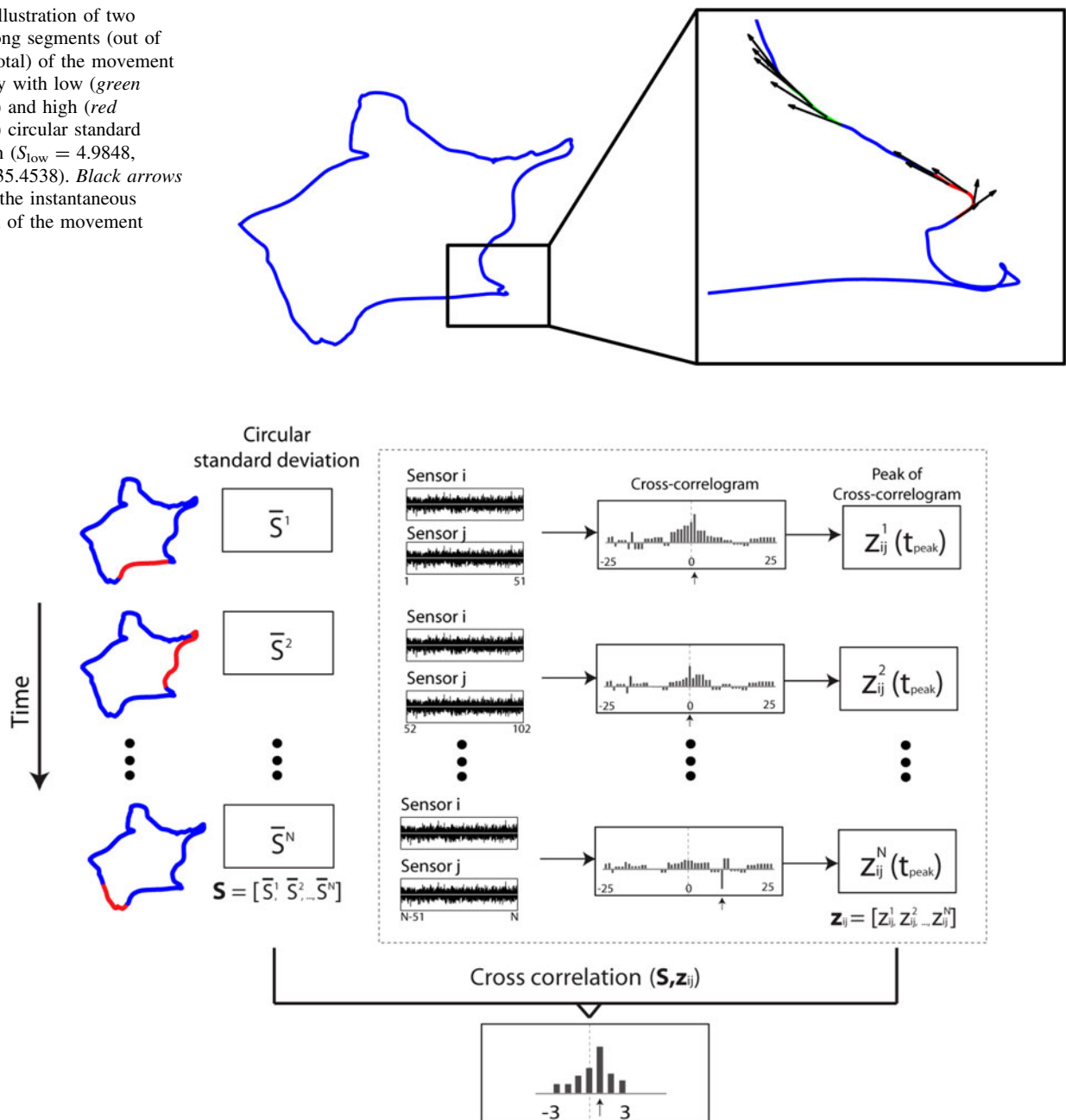


**Fig. 2** The flowchart of the technique used to assess the relation between neural interactions and variability of movement direction (see “Methods” section for more details)

the cross-correlation occurred, because it indicates whether neural interactions precede (i.e., negative time-lags) or follow (i.e., positive time-lags) changes in movement direction. Note that in a control theory context, negative and positive time-lags are related to feedforward and feedback motor processes, respectively (Box et al. 2008). Feedforward motor control processes are related to planning and execution of movements, whereas feedback motor

control processes are associated with error-correction of movements.

We are interested in identifying the cortical regions that contribute the most to feedforward and feedback processes. To accomplish this, we counted the number of positive ( $p$ ) and negative ( $n$ ) time-lags  $t_{\text{peak}}$ , for each sensor with the rest of 247 sensors, across all subjects. If there were more negative than positive time-lags, we considered that this



sensor is related mostly to a feedforward control scheme; otherwise, it was considered to contribute mostly to a feedback control scheme.

#### Comparison of neural interactions between straight and curved movements

We were also interested in testing whether there are any differences in neural interactions between straight and curved movements in the copying task. To test that, we classified the time-bins into two groups based on the circular standard deviation: (1) time-bins with low  $\bar{S}$  (straight movements) and (2) time-bins with high  $\bar{S}$  (curved movements). The time-bins were categorized based on the histogram mean of  $\bar{S}$  for each subject. A time-bin was placed in group 1 if  $\bar{S}$  was less than 20 % of the histogram mean; otherwise, it was placed in group 2. Although this threshold was selected somewhat arbitrarily, trajectory segments with  $\bar{S}$  less than 20 % of the histogram mean were almost straight movements with substantially low directional variability. Other threshold values (e.g., 15 and 25 %) were also tested in this analysis and gave similar results. We then performed a two-sample  $t$  test for each pair of sensors between the two groups and used the  $P$  value for the group factor as a quantitative measure of the magnitude of the effect of the directional variability of movement on the neural interactions.

#### *Spatial distribution of sensors related to feedforward and feedback processes*

We used the difference between the positive ( $p$ ) and negative ( $n$ ) time-lags  $t_{\text{peak}}$  for each sensor to estimate the spatial frequency distribution of the cortical areas that contribute the most to feedforward and feedback motor control processes. In particular, we visualized the absolute difference between  $n$  and  $p$  for each sensor that contribute the most to the feedforward scheme with intermediate values interpolated using MATLAB<sup>®</sup> functions: *patch*, and *convhulln* (see Fig. 7). The color intensity is proportional to the different  $n - p$  (blue areas correspond to near-zero differences and red areas correspond to high differences). In a similar way, we handle the sensors associated with the feedback scheme ( $p - n > 0$ ) (see Fig. 8).

#### *Spatial distribution of sensors related to changes in movement direction*

In a similar manner, we plotted the spatial distribution of the sensors that exhibit differences in interactions with other sensors between straight and curved movements, using the probability value of the two-sample  $t$  test as a

quantitative measure of the magnitude of the effect in sensor space. For this analysis, we used the log-transformation of the probability value  $P$  to normalize its distribution (i.e.,  $P' = -\ln P$ ). This procedure generates images in a similar way to a fixed-effect analysis across all subjects in fMRI studies. However, the difference with the statistical parametric mapping (SPM) in fMRI is that instead of using the  $t$  statistics from the average subject's activation, we are using the maximum  $P'$  related to a specific sensor (out of 247 possible) (see Fig. 9).

## Results

### MEG cross-correlation analysis

From the 248 MEG sensors, we produced  $\binom{248}{N} \times N$  time-bins  $\times$  10 subjects cross-correlograms and normalized them using Fisher's  $z$ -transformation (see "Methods" section) before averaging across subjects. We characterized the cross-correlogram by computing the sign and the strength of the peak cross-correlation  $z_{ij}(t_{\text{peak}})$  and the time-lag  $t_{\text{peak}}$  at which the peak of cross-correlation occurred. Of the 259,419,160  $z_{ij}(t_{\text{peak}})$ , 50.56 % were positive and 49.44 % were negative. The average (mean  $\pm$  SEM) positive  $z_{ij}(t_{\text{peak}})$  was  $0.3235 \pm 5.2831 \times 10^{-6}$  (maximum  $z_{ij}(t_{\text{peak}}) = 1.4862$ ;  $cc_{ij}(t_{\text{peak}}) = 0.9026$ ); the average negative  $z_{ij}(t_{\text{peak}})$  was  $-0.3222 \pm 5.2346 \times 10^{-6}$  (minimum  $z_{ij}(t_{\text{peak}}) = -0.9774$ ;  $cc_{ij}(t_{\text{peak}}) = -0.7519$ ). Additionally, we found that 12,471,286 out of 259,419,160 (4.8074 %)  $z_{ij}(t_{\text{peak}})$  had the peak of cross-correlation at zero-lag and the rest (95.1926 %) at non-zero-lag.

### Behavioral data analysis

We divided the XY joystick movement trajectory in 51 ms time-bins and computed the local circular standard deviation  $\bar{S}$  of the movement direction within each time-bin to characterize the directional variability of the movement. The relative frequency distribution of  $\bar{S}$  across all time-bins and subjects is presented in Fig. 3a. To make the distribution more symmetric and homoscedastic, we computed the log-transformation of  $\bar{S}$ , Fig. 3b.

### Relation between neural interactions and variability of movement direction

To look at the relationship between neural interactions and the directional variability of the movement, we computed the cross-correlation function (CCF) between the time series of  $z_{ij}(t_{\text{peak}})$  (absolute value) and the prewhitened

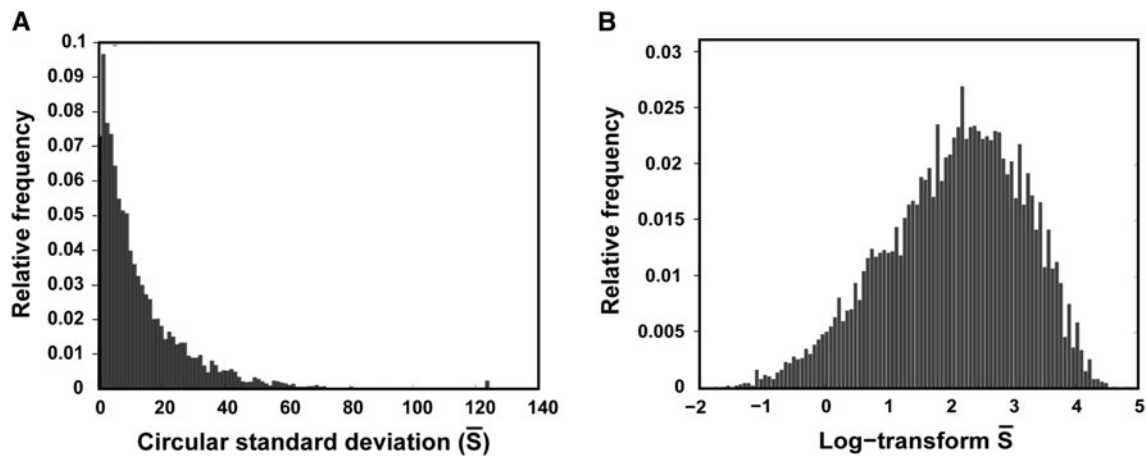


**Fig. 3** **a** Relative frequency distribution of the circular standard deviation,  $\bar{S}$ , of movement direction for 51-ms trajectory segments, across all time-bins and subjects (8,460). **b** Relative frequency distribution of the  $\bar{S}$  log-transformation

log-transformed  $\bar{S}$  over  $\pm 3$  time-lags including zero-lag (1 time-lag corresponds to  $\pm 25$  time-lags in the cross-correlation analysis of the MEG time series). Altogether, 306,280 (30,628 pairs of MEG sensors  $\times$  10 subjects) cross-correlograms were available for further analysis. We characterized the cross-correlograms by computing the sign and the strength of the peak cross-correlation  $z_{ij}^s(t_{\text{peak}})$  and the corresponding lag  $t_{\text{peak}}$  at which the peak occurred. Of the 306,280  $z_{ij}^s(t_{\text{peak}})$ , 153,561 (50.14 %) were positive and 152,719 (49.86 %) were negative. The average (mean  $\pm$  SEM) positive  $z_{ij}^s(t_{\text{peak}})$   $0.0593 \pm 4.6996 \times 10^{-5}$  (maximum  $z_{ij}^s(t_{\text{peak}}) = 0.1662$ ,  $cc_{ij}^s(t_{\text{peak}}) = 0.1647$ ); the average negative  $z_{ij}^s(t_{\text{peak}})$  was  $-0.0593 \pm 4.7199 \times 10^{-5}$  (minimum  $z_{ij}^s(t_{\text{peak}}) = -0.1672$ ;  $cc_{ij}^s(t_{\text{peak}}) = -0.1657$ ). The relative frequency distribution of  $cc_{ij}^s(t_{\text{max}})$  across pairs of sensors and subjects is illustrated in Fig. 4a.

Next, we focus the analysis on the time-lag  $t_{\text{peak}}$ , at which the peak of the cross-correlation occurred. We found 43,798 (14.30 %) cross-correlograms had their peak at zero-lag, 131,008 (42.77 %) at negative-lag and 131,474 (42.93 %) at positive lag. Zero-lag indicates synchronous association between neural interactions and directional variability of movement. On the other hand, positive or negative-lag corresponds to asynchronous interactions, in which one variable drives the other. Specifically, negative-lag denotes that modulations in neural interactions precede changes in movement direction and vice versa for positive lag. The relative frequency distribution presented in Fig. 4b shows that  $t_{\text{peak}}$  is almost uniformly distributed between  $\pm 3$  lags. We interpret these results as evidence that neural interactions vary with the movement direction in a feedforward–feedback control scheme. We can visualize the neural interactions associated with feedforward

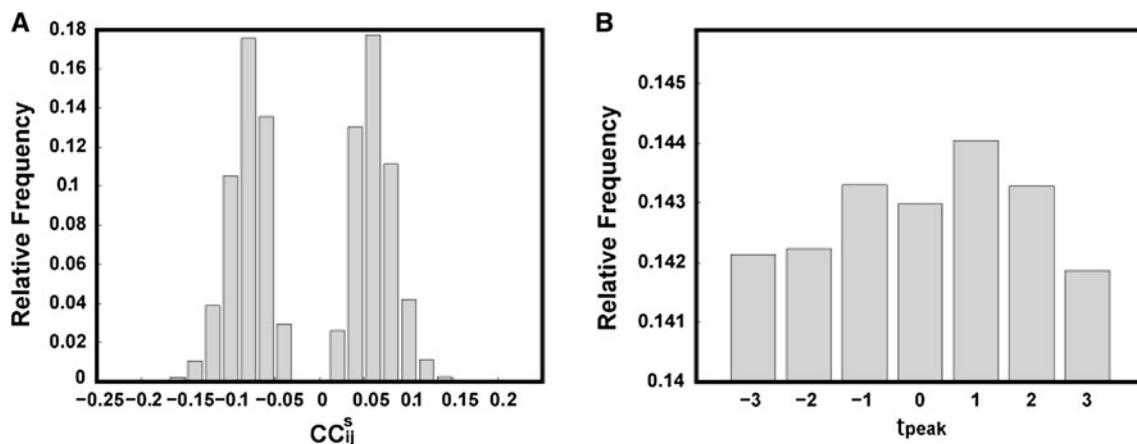


**Fig. 4** **a** Relative frequency distribution of the peak cross-correlations between the strength of neural interactions and the circular standard deviations across all pairs of sensors and subjects (306,280).

**b** Relative frequency distribution of  $t_{\text{peak}}$ , which corresponds to the time-lags that peak of cross-correlations occurred

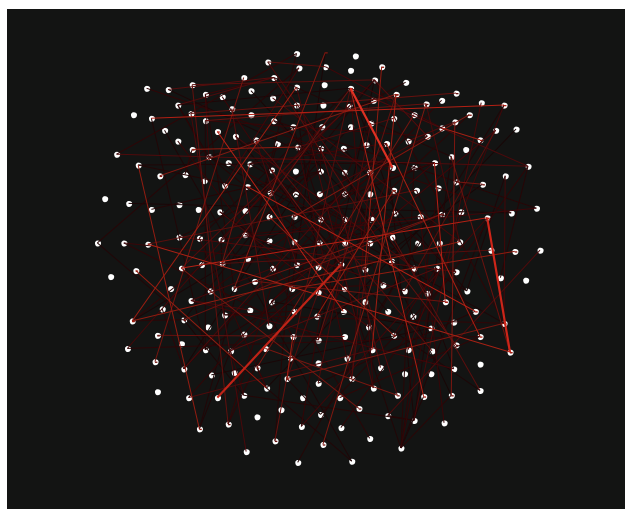


**Fig. 5** Massively interconnected “feedforward” network, averaged across the 10 subjects. The *red lines* denote sensor interactions that are correlated with the circular standard deviation at negative time-lags. The *color intensity* of a *line* is proportional to the strength of coupling between the sensors interactions and the circular standard deviation

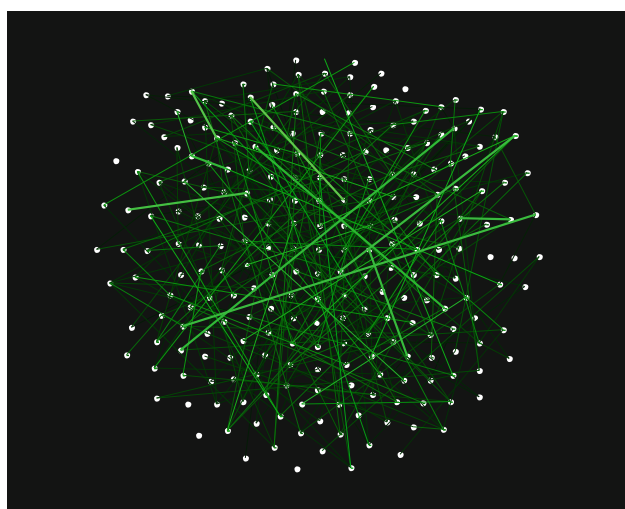


**Fig. 6** Massively interconnected “feedback” network, averaged across the 10 subjects. The *green lines* denote sensor interactions that are correlated with the circular standard deviation at positive time-lags. The *color intensity* of a *line* is proportional to the strength of coupling between the sensors interactions and the circular standard deviation

and feedback control mechanisms by connecting the 248 MEG sensors with red and green lines, respectively. Figures 5 and 6 illustrate a thresholded ( $p < 5 \times 10^{-4}$ ) and scaled view of these networks across the 10 subjects. Notice the frequent intra and interhemispheric interactions in both “feedforward” and “feedback” networks. The spatial distribution of the sensors that contribute the most in the feedforward control scheme is presented in Fig. 7. Particularly, Fig. 7a depicts a flattened two-dimensional (2D) contour plot, whereas Fig. 7b–d shows the right, left,

and rare views of a 3-D plot. Similarly, the spatial distribution of the sensors that contribute the most in feedback control scheme is presented in Fig. 8. The results showed a strong focus of sensors associated with the feedforward scheme in the left hemisphere (contralateral to the moving hand)—left inferior frontal gyrus (IFG) (A), left superior temporal gyrus (STG) (B), and left cerebellar hemisphere (C)—and the right occipital–temporal junction (D). On the other hand, sensors associated with the feedback scheme are localized in the right posterior parietal cortex (PPC) (E), left cerebellar hemisphere (F), and the right lateral occipital area (LO) (G). These areas were estimated based on the 3-D sensor layout in the MEG helmet and typical brain surface reconstructions from brain MRIs using the integrated BESA (version 5.06, MEGIS Software GmbH, Gräfelfing, Germany) and Brain Voyager (Electrical Geodesics, Inc., Eugene OR, USA), package.

#### Two-sample *t* test between “low” and “high” directional variability groups

We explored whether there are any differences in neural interactions between trajectory segments with low (i.e., straight movements) and high (i.e., curved movements) variability of movement direction. Figure 9a, b depicts the log-transformed (i.e.,  $-\ln P$ ) probability value of the two-sample *t* test across all subjects for each sensor, in a flattened two-dimensional (2D) contour plot and a 3-D plot, respectively (see “Methods” section). The color intensity is proportional to the maximum  $-\ln P$  related to the specific sensor (out of 247 possible). The results showed a preponderance of sensors with stronger effects over the right hemisphere—ipsilateral to the moving hand. These sensors are closest to right superior temporal gyrus (A) and the right occipital cortex (B) and exhibit stronger coupling with the rest of the sensors for trajectory segments with high rather than low directional movement variability.

## Discussion

### Overview

We used Box–Jenkins (Jenkins and Watts 1968; Box et al. 2008) time series analysis to account for dynamic coupling between MEG stationary time series interactions and directional variability of movement, in a continuous and sequential copying task. Our hypothesis was that interactions between brain areas are associated with movement direction. The neural interactions can be estimated by correlating time courses of the MEG signals recorded from different sensors. However, the time courses of the MEG raw data are typically non-stationary and highly autocorrelated, and thus, the



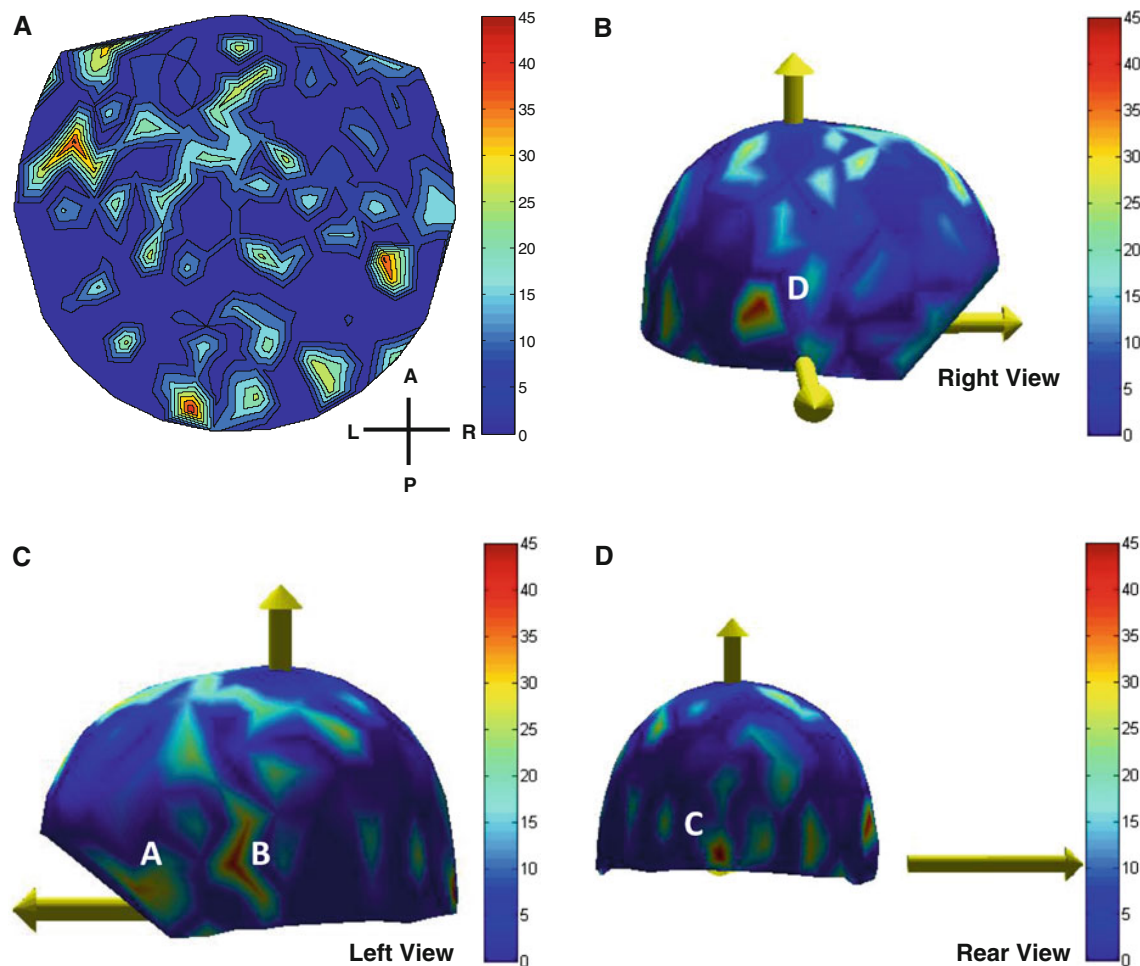


**Fig. 7** **a** 2-D Spatial distribution of the sensors involved mostly in the feedforward scheme. The *color codes* the difference between negative ( $n$ ) and positive ( $p$ ) time-lag  $t_{\text{peak}}$  related to the specific sensor (out of 247 possible), interpolated linearly in sensor space.

**b** Right, **c** left and **d** rear view of the 3-D surface plot using Delaunay triangulation of MEG sensor coordinates with interpolated, color-coded  $n - p$  values

cross-correlation analysis could lead to spurious and erroneous results (Jenkins and Watts 1968; Granger and Newbold 1974, 1977; Priestley 1981; Box et al. 2008). The remedy is to render the time series stationary and non-autocorrelated for the cross-correlation to be valid (i.e., no spurious) assessments of interactions. This preprocessing is called “prewhitening” of the time series and is typically accomplishing by fitting an ARIMA model to the raw data and taking the residuals.

To explore the association between neural interactions and variability of movement direction, we divided the recording session into time-bins of 51 time-steps and computed all possible pairwise lagged cross-correlations within each time-bin using the prewhitened MEG time series. We characterized each of the cross-correlograms by computing the sign and the peak of the cross-correlation and the corresponding time-lag. Additionally, we estimated the directional variability of the movement within each time-bin, by computing the circular standard deviation of

the movement direction. The directional variability of the movement provides an estimate of whether the current trajectory segment is a straight or a curved movement.

The relation between neural interactions and directional variability of the movement was assessed separately for each pair of sensors by correlating the time series of the strength of the peak MEG cross-correlations and the time series of circular standard deviations. The results showed that neural interactions and directional variability of the movement are coupled in an action-correction scheme (i.e., feedforward–feedback control). Particularly, we found sensor interactions that precede (i.e., feedforward) or follow (feedback) the changes in movement direction. The sensors associated with feedforward processes are localized in the left IFG, the left STG, left cerebellar hemisphere, and the right occipito–temporal junction. On the other hand, the main loci of sensors associated with feedback processes are in right PPC, right LO area, and left cerebellar hemisphere. Additionally, we tested whether there is

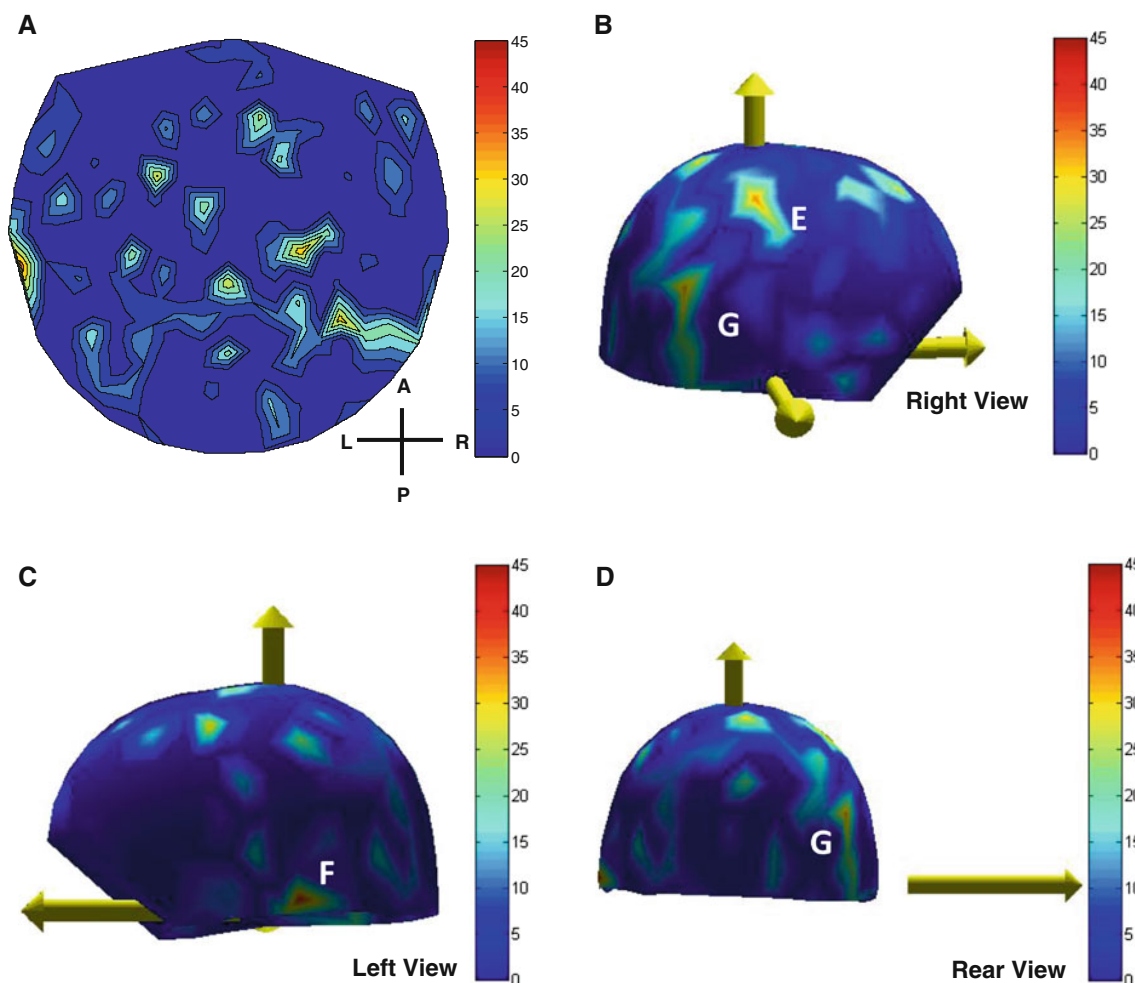


**Fig. 8** **a** 2-D Spatial distribution of the sensors involved mostly in the feedback scheme. The *color codes* the difference between positive ( $p$ ) and negative ( $n$ ) time-lag  $t_{\text{peak}}$  related to the specific sensor (out of

247 possible), interpolated linearly in sensor space. **b** Right, **c** left and **d** rear view of the 3-D surface plot using Delaunay triangulation of MEG sensor coordinates with interpolated, color-coded  $p - n$  values

any difference in neural interactions between movements with low and high directional variability. Interestingly, we found sensors around the right hemisphere, which showed stronger coupling with the rest of the sensors for trajectory segments with high rather than low directional variability.

#### Feedforward–feedback control processes

The involvement of specific cortical regions in feedforward processes is in line with a series of neurophysiological and functional neuroimaging studies in copying and tracing shapes. Moran and Schwartz measured the time interval between neural activity of cells in premotor and motor cortices and the movement in a spiral tracing task (Moran and Schwartz 1999b). They found that neural activity in these cortical areas precedes the hand movement by several milliseconds and scales with the curvature of the movement trajectory. Additionally, dipole analysis of the MEG signals performed previously in our laboratory revealed

consistent dipoles locations in various brain regions included the left motor cortex, parietal cortex, frontal and temporal regions, and the occipital cortex (Langheim et al. 2005). Interestingly, most of the STG dipoles were found in time points preceding the corners (i.e., prior to change movement direction), suggesting that this region is involved in feedforward motor control processes. Our finding that sensors contributing to the feedforward networks are also distributed in the IFG area is consistent with the results from functional neuroimaging studies that showed that this area is involved in both copying geometrical shapes (Krams et al. 1998) and observing these shapes prior to the copying task (Tzagarakis et al. 2009).

The involvement of the PPC area in feedback motor control processes is in line with a series of previous neurophysiological and clinical studies (see the review by Buneo and Andersen 2006). Ashe and Georgopoulos (1994) explored the time course of the ongoing cell activity in relation to evolving motor parameters for 2-dimensional

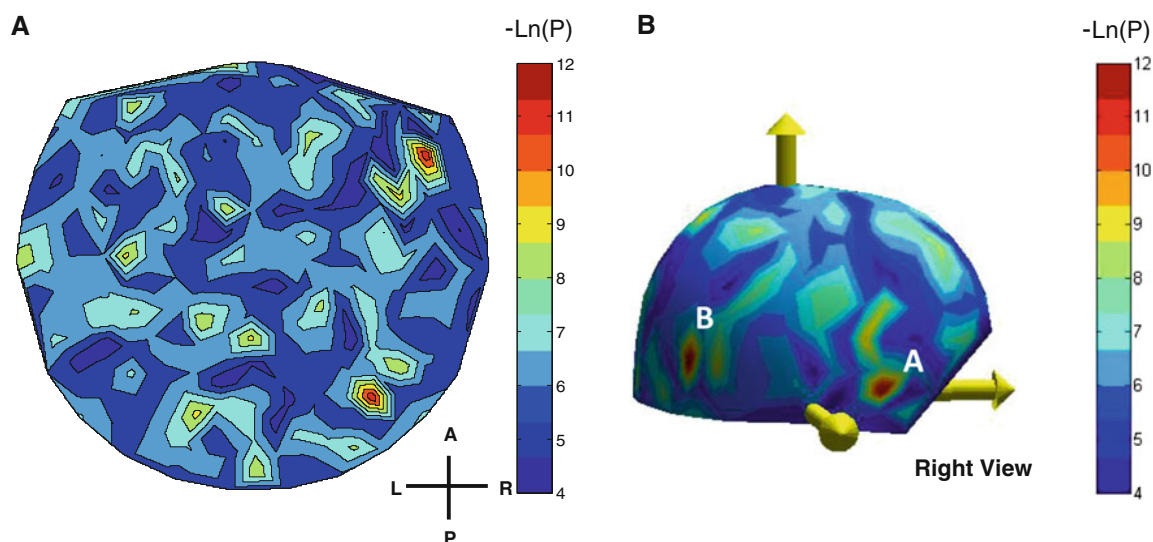


**Fig. 9** **a** 2-D contour plot of color-coded two-sample  $t$  test  $-\ln P$  values, interpolated linear in sensor space for low versus high directional movement variability. **b** 3-D surface plot using Delaunay

triangulation of MEG sensor coordinates with interpolated, color-coded two-sample  $t$  test  $-\ln P$  values for low versus high directional movement variability

movements made toward 8 visual targets. They found that the timing of the highest correlation (i.e., highest  $R^2$ ) between firing rates and ongoing movement trajectories in motor cortex and PPC (area 5) were  $-90$  and  $+30$  ms, respectively (Ashe and Georgopoulos 1994). Clinical studies provide evidence that PPC is involved in error detection and correction by comparing the differences between the actual position of the hand and the goal position. Particularly, patients with PPC damage are able to plan reaching movements accurately to stationary objects, but they failed to correct the movement when the position of the objects changes unexpectedly (Grea et al. 2002). Disruption of the parietal cortex in healthy individuals using transcranial magnetic stimulation (TMS) produces similar behavioral deficits in reaching movements with unpredictable changes in goal position (Desmurget et al. 1999).

An interesting finding in our analysis is that sensors that are mostly involved in feedback processes are also distributed around the right occipital lateral area, despite the absence of novel visual stimulus and eye movements. However, dipole analysis in the MEG signals found dipoles in the occipital cortex in time points following the corners (i.e., the changes in movement direction). This finding suggests that the visual cortex may have been utilized within a network of cortical regions to continuously update the motor template in subjects during the copying task (Langheim et al. 2005).

Except for cortical areas, which are involved mainly in either feedforward or feedback processes, we found that the left cerebellar hemisphere is involved in both motor control

processes. This finding is consistent with a series of motor control studies, which showed that the cerebellum is required for predicting sensory outcomes of actions and compensating of ongoing motor commands (Bastian 2006; Nowak et al. 2007). This theory is also supported by clinical studies in patients with cerebellum damage that encounter significant difficulties in learning new tools and adapting their behavior to unpredictable changes (Nowak et al. 2007). Additionally, several computational (Kawato and Gomi 1992; Houk et al. 1996) and functional imaging studies (Miall et al. 2000; Van Mier and Petersen 2002) proposed that activation in the cerebellum is associated with error-based learning tasks. Particularly, Van Mier and Petersen found a strong correlation between decreases in cerebellum activity in left hemisphere and decreases in errors in a tracing task, suggesting that activation in the left cerebellum might be related to error detection and correction (Van Mier and Petersen 2002).

Overall, our results enhance findings from previous experiments, mainly clinical and electrophysiological studies, that particular cortical areas are involved in planning and error-correction in movements. Unlike these studies, which are limited in exploring only specific brain areas, the novelty of our study is that we looked at the “whole brain” and estimated the areas that contribute in action-correction by correlating neural interactions with a behavioral control parameter. To the best of our knowledge, this is the first study that shows how neural interactions are associated with a behavioral control parameter in continuous and sequential movements.

## Neural interactions related to straight and curved movements

We were also interested in studying the potential differences in neural interactions between straight and curved movements. Electrophysiological studies explored the association between neural activity and hand movement in visuomotor tasks recording from motor and premotor cortices and found that the time-lag between neural activity and hand movement varies linearly with the instantaneous radius of the trajectory's curvature—the time-lag is longer when the trajectory is more curved (Schwartz 1994; Moran and Schwartz 1999b). These results suggest that for straight movements, a “keep moving the same direction” signal transmitted once is more efficient than continuous transmission of the same direction. Once the movement direction changes rapidly over a short period of time, more processing time is required, increasing the time interval between neural activity and hand movement. These studies focused only on the premotor and motor cortices due to the inherent limitation of electrophysiological techniques, whereas they did not provide any information on whether and how neural interactions vary with the curvature of the movement trajectory.

In the current study, we tested whether the neural interactions vary between straight and curved movements. To test that, we categorized the time-bins of the recordings into two groups based on the directional variability of 51-ms trajectory segments—that is, a group with low directional variability (i.e., straight movements) and a group with high directional variability (curved movements). We tested whether the neural interactions are different between the two groups and found pairs of MEG sensors that have different interaction strengths between straight and curved movements. Interestingly, the preponderance of these sensors is distributed over the right hemisphere—ipsilateral to the moving hand—and specifically around the superior temporal gyrus and right occipital cortex. These sensors showed strongest coupling with the rest of the sensors for trajectory segments with high rather than low directional variability of movement—that is, for curved rather than straight movements. Although these results might seem counterintuitive, since all participants were right handed, they complement results from previous studies, which showed that cortical areas ipsilateral to the hand movement are recruited for movements with higher indices of difficulty in comparison with simple movements. For instance, studies in sequential movements showed ipsilateral motor cortex recruitment when subjects performed complex movements in comparison with simple finger flexion tasks (Rao et al. 1993; Salmelin et al. 1995). Similarly, we can argue that the index of difficulty in a sequential copying task is higher for changing direction

than moving in a straight path, and hence, the difference in neural interactions between curved and straight movements is represented mainly in the ipsilateral hemisphere.

**Acknowledgments** This study was supported by the American Legion Brain Sciences Chair and the US Department of Veterans Affairs. We thank Dr. J. Bonaiuto for comments on the manuscript and for discussions.

## References

- Andres FG, Mima T, Schulman AE, Dichgans J, Hallett M, Gerloff C (1999) Functional coupling of human cortical sensorimotor areas during bimanual skill acquisition. *Brain* 122:855–870
- Ashe J, Georgopoulos AP (1994) Movement parameters and neural activity in motor cortex and area 5. *Cereb Cortex* 4:590–600
- Averbeck BB, Chafee MV, Crowe DA, Georgopoulos AP (2003) Neural activity in prefrontal cortex during copying geometrical shapes. I. Single cells encode shape, sequence, and metric parameters. *Exp Brain Res* 150:127–141
- Averbeck BB, Crowe DA, Chafee MV, Georgopoulos AP (2009) Differential contribution of superior parietal and dorsal-lateral prefrontal cortices in copying. *Cortex* 45:432–441
- Bastian AJ (2006) Learning to predict the future: the cerebellum adapts feedforward movement control. *Curr Opin Neurobiol* 16:645–649
- Box GEP, Jenkins GM, Reinsel GC (2008) Time series analysis: forecasting and control. Holden Day, San Francisco
- Buneo CA, Andersen RA (2006) The posterior parietal cortex: sensorimotor interface for the planning and online control of visually guided movements. *Neuropsychologia* 44(13):2594–2606
- Caminiti R, Chafee MV, Battaglia-Mayer A, Averbeck BB, Crowe DA, Georgopoulos AP (2010) Understanding the parietal lobe syndrome from a neurophysiological and evolutionary perspective. *Eur J Neurosci* 31:2320–2340
- De Renzi E (1982) Disorders of space exploration and cognition. Elsevier, Amsterdam
- Desmurget M, Grafton S (2000) Forward modeling allows feedback control for fast reaching movements. *Trends Cogn Sci* 4: 423–431
- Desmurget M, Epstein CM, Turner RS, Prablanc C, Alexander GE, Grafton S (1999) Role of the posterior parietal cortex in updating reaching movements to a visual target. *Nat Neurosci* 2:563–567
- Gerloff C, Richard J, Hadley J, Schulman AE, Honda M, Hallett M (1998) Functional coupling and regional activation of human cortical motor areas during simple, internally paced and externally paced finger movements. *Brain* 121:1513–1531
- Gevins AS, Schaffer RE, Doyle JC, Cuttillo BA, Tannehill RS, Bressler S (1983) Shadows of thought: shifting lateralization of human brain electrical patterns during brief visuomotor task. *Science* 220:97–99
- Granger CWJ, Newbold P (1974) Spurious regressions in econometrics. *J Econom* 2:111–120
- Granger CWJ, Newbold P (1977) Forecasting economic time series. Academic, New York, NY
- Grea H, Pisella L, Rossetti Y, Desmurget M, Tilikete C, Grafton S, Prablanc C, Vighetto A (2002) A lesion of the posterior parietal cortex disrupts on-line adjustments during aiming movements. *Neuropsychologia* 40:2471–2480
- Grol MJ, Majdandžić J, Stephan KE, Verhagen L, Dijkerman HC, Bekkering H, Verstraten FA, Toni I (2007) Parieto-frontal connectivity during visually guided grasping. *J Neurosci* 27: 11877–11887

- Houk JC, Buckingham JT, Barto AG (1996) Models of the cerebellum and motor learning. *Behav Brain Sci* 19:368–383
- Jenkins GM, Watts DG (1968) Spectral analysis and its applications. Holden Day, San Francisco
- Kawato M, Gomi H (1992) A computational model of four regions of the cerebellum based on feedback-error learning. *Biol Cybern* 68:95–103
- Krams M, Rushworth MF, Deiber MP, Frackowiak RS, Passingham RE (1998) The preparation, execution and suppression of copied movements in the human brain. *Exp Brain Res* 120:386–398
- Langheim FJ, Merkle AN, Leuthold AC, Lewis SM, Georgopoulos AP (2005) Dipole analysis of magnetoencephalographic data during continuous shape copying. *Exp Brain Res* 170:513–521
- Leuthold AC (2003) Subtraction of heart artifact from MEG data: the matched filter revisited. *Soc Neurosci Abstr* 863.15
- Leuthold AC, Langheim FJ, Lewis SM, Georgopoulos AP (2005) Time series analysis of magnetoencephalographic data during copying. *Exp Brain Res* 164:411–422
- Luria AR, Tsvetkova LS (1964) The programming of constructive activity in local brain injuries. *Neuropsychologia* 2:95–107
- Miall RC, Imamizu H, Miyauchi S (2000) Activation of the cerebellum in co-ordinated eye and hand tracking movements: an fMRI study. *Exp Brain Res* 135:22–33
- Moran D, Schwartz AB (1999a) Motor cortical representation of speed and direction during reaching. *J Neurophysiol* 82: 2676–2692
- Moran DW, Schwartz AB (1999b) Motor cortical activity during drawing movements: population representation during spiral tracing. *J Neurophysiol* 82:2693–2704
- Nowak DA, Timmann D, Hermsdörfer J (2007) Dexterity in cerebellar agenesis. *Neuropsychologia* 45:696–703
- Priestley MB (1981) Spectral analysis and time series. Academic, San Diego, CA
- Rao SM, Binder JR, Bandettini PA, Hammeke TA, Yetkin FZ, Jesmanowicz A, Lisk LM, Morris GL, Mueller WM, Estokowski LD et al (1993) Functional magnetic resonance imaging of complex human movements. *Neurology* 43:2311–2318
- Salmelin R, Forss N, Knuutila J, Hari R (1995) Bilateral activation of the human somatomotor cortex by distal hand movements. *Electroencephalogr Clin Neurophysiol* 95:444–452
- Schwartz AB (1994) Direct cortical representation of drawing. *Science* 265:540–542
- Seidler RD, Noll DC, Thiers G (2004) Feedforward and feedback processes in motor control. *Neuroimage* 22:1775–1783
- Shadmehr R, Krakauer JW (2008) A computational neuroanatomy for motor control. *Exp Brain Res* 185:359–381
- Toma K, Mima T, Matsuoka T et al (2002) Movement rate effect on activation and functional coupling of motor cortical areas. *J Neurophysiol* 88:3377–3385
- Tzagarakis C, Jerde TA, Lewis SM, Uğurbil K, Georgopoulos AP (2009) Cerebral cortical mechanisms of copying geometrical shapes: a multidimensional scaling analysis of fMRI patterns of activation. *Exp Brain Res* 194:369–380
- Van Mier HI, Petersen SE (2002) Role of the cerebellum in motor cognition. *Ann N Y Acad Sci* 978:334–353
- Wu W, Gao Y, Bienenstock E, Donoghue JP, Black MJ (2006) Bayesian population decoding of motor cortical activity using a kalman filter. *Neural Comput* 18:80–118